Effects of Potentials on the Vibrational Dynamics of Ice

Jichen Li

Department of Physics, UMIST, P.O. Box 88, Manchester M60 1QD, U.K.

Received: October 11, 1996; In Final Form: May 20, 1997[⊗]

Since the observation of the molecular optic peaks at 28 and 37 meV in the inelastic by using inelastic neutron scattering spectra for ice Ih,[1] reproducing the double-peak feature is presenting considerable challenge and controversy. Although there are a number of lattice and molecular dynamic calculations in the literature, none of them can reproduce the complete integrated phonon density of states to match the features seen in the neutron scattering spectra. Our lattice dynamical model[1] shows that two quite distinct hydrogen bond force constants are required in order to reproduce the measured phonon density of states. In this paper, we try to examine the dynamical properties of the existing potentials and to resolve some of the issues related to this topic.

1. Introduction

Water and its solutions are subjects that have been extensively studied in recent decades. The importance of these studies is due not only to the fact that water is the most important substance on Earth and in living organisms but also because its many "anomalous" properties were and are continuously attracting scientific attention. Despite the great efforts that have been devoted to the problem, we are still far from understanding its complex microscopic properties. The fundamental problem lies in our understanding of the H-bond interaction. In the last 30 years, a large number of pair potentials for water have been proposed, some empirical and some based on ab initio quantum mechanical calculations of water dimers. Validating these pair potentials is still a controversial area, and no consensus has been reached regarding which potential is the most suitable one for water/ice in general.

The development of high-intensity, high-resolution, inelastic neutron scattering instruments has recently made it possible for this technique to match the precision of IR and Raman measurements for ices. The aim of the studies is to provide a way of testing the existing potentials. Our earlier investigation for ice Ih/Ic shows the surprising feature in the measured spectrum of the presence of two sharp triangular features in the translational mode region for ice Ih with a high-energy cutoff at about 28 meV (225 cm^{-1}) and 37 meV (298 cm^{-1}).[1] The high-energy peak at 37 meV has an area (or integrated intensity) twice as big as the low-energy peak at 28 meV. These areas are directly proportional to phonon density of states (PDOS) weighted by the mean square amplitude associated with all the modes integrated over the first Brillouin zone (BZ). Although these features were detectable in earlier neutron measurements, it had not previously been realized that they were so well separated. In order to reproduce these inelastic incoherent neutron scattering (IINS) spectra, we have proposed a model, which differs from the existing theories. Hence this model has caused considerable controversy in this field. The model is based on a hypothesis: two strengths of hydrogen bonding in ice[1] (i.e. Li−Ross hypothesis). One important question is whether it is necessary to invoke such a radical model; that is, are the current potentials capable of giving the properties of measured inelastic incoherent neutron scattering spectra? To answer this question, we need to examine the existing potentials for water and the current state of our understanding of the vibrational dynamics of ice.

2. Water−Water Potentials

One of the abnormal features related to this subject is that many water−water pair potentials exist. Some of the potentials may be good at reproducing structural properties of water; others may be good at reproducing density and a range of other thermodynamical properties. Extensive studies of these potentials have been made by comparing the structures of water[2] and of ice[3] produced by these potentials. Looking at the evolution of the water−water potential development, one can see that the progress of the potentials is associated with a gradual process of increasing their anisotropic properties from very early simple Lennard-Jones type to more complicated polarized potentials in order to account for the various water properties. Figure 1 plots one of the common potentials used in the structural simulations, the MCY potential.[4] It consists of an exponential hard-core and three point charge interactions, which gives small orientational differences in the bonding energy and force constants along the different orientations for the different configurations in ice Ih[1] (see Table 1). Most of these potentials (listed in Table 1) are, in general, capable of stabilizing a structure of water and ice. However, good agreement between experimental structure factors and those simulated using these potentials requires a delicate balance of many competing effects, such as the short-range interactions from the core part of the potentials against the long-range charge interactions, and the effect from angle dependent terms against distance dependent terms. Small changes in the arrangement of the charges (as in the three-point and four-point charge models) could result in significant changes in the final structure reproduced from the potentials. These collective effects are impossible to separate from one another, which makes it hard for us to come to a consensus and finalize a potential acceptable for a large number of users.

On the other hand, validating these potentials so far is limited to the area of structural related subjects. There are few tests of their suitability for producing the right phonon frequencies. In fact, spectroscopic measurements of the vibrational spectrum are the most powerful way of investigating the effective potentials for a given system, because the frequencies of the vibrational modes are determined by the interatomic forces, which are determined by the double differentials of the

[⊗] Abstract published in *Advance ACS Abstracts,* July 1, 1997.

S1089-5647(96)03276-2 CCC: $14.00

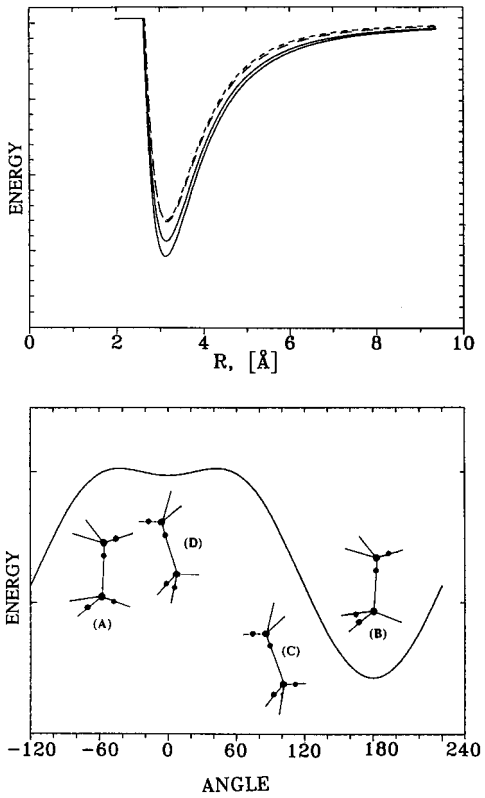

Figure 1. Plot of the four different orientations of the MCY potential: the lower diagram is a plot of the banding energy vs relative water dipole−dipole angle. The configurations are indicated in the inserted diagrams; for instance, the B configuration at 180° corresponds to the lowest energy configuration. The upper diagram is a plot of total energy vs O−O separation distance *r*, and the second lowest continuous curve corresponds to the C configuration at 120°, while the two dashed lines correspond to A (at 60°) and D configurations (at 0°).

potentials. Therefore, measuring the vibrational frequencies of the system provides a better way to examine the potential in a more detailed manner. This will require lattice dynamic or molecular dynamic calculations. Table 1 lists the basic properties of some known potentials that relate to the phonon calculations.

3. Vibrational Dynamics of Ice

The vibrational spectrum of ice can be simulated by either lattice dynamic (LD) or molecular dynamic (MD) methods. In the LD approach, the calculation begins with the adiabatic approximation, which enables us to treat the solutions in the electronic problem as interaction potentials in the nuclear problem. By assuming harmonic forces and periodic boundary conditions, we can obtain a normal mode distribution function of the nuclear displacements. The problem is then reduced to a classic system of coupled oscillators. Under these conditions the one-phonon dispersion relation can be evaluated, and hence the one-phonon density of states can be calculated. On the other hand, the MD calculations are based on numerically integrating Newton's equations for a multibody system. Then the Fourier transformation of the velocity autocorrelation function will yield the PDOS. Because of the self-convolution of the velocity involved in the MD calculations, it is essentially the same as IINS measurements: intensity is proportional to the displacement of each individual atom (or molecule); it is therefore most suitable for interpreting the data obtained from IINS.

In the past, the spectrum for ice Ih has been frequently calculated by using LD and MD techniques. In the early 1970s, Shawyer and Dean[5] used a simple force constant LD model to calculate the spectrum of ice Ih (up to 3500 cm^{-1}). In their model, only the nearest neighbor interactions were taken into account by using a range of force constants, which are listed in Table 2. The proton disordering was also considered by using large supercells up to 500 molecules. The aim of their calculations was to fit the infrared absorption data obtained by Bertie et al. (1969). Hence one optic molecular peak was generated at ∼220 cm^{-1} (see Figure 2), which matched the experimental data well. Later, Wong and Whalley[6] had improved Shawyer and Dean's calculation by introducing dipole−dipole interactions. As there are four different local proton arrangements (see Figure 1), four different O−O stretching force constants were therefore used (see Table 2). However, because the contributions from the dipole moments are relatively small in comparison with the basic O−O strength force constant, the resulting PDOS are very similar to Shawyer and Dean's calculation in the translational region. Since IINS spectra have been available, scientists have realized that the peak at ∼300 cm^{-1} is also composed of one-phonon fundamental modes which have to be represented in the LD calculations. There is, therefore, a requirement to improve the existing LD model in order to reproduce the two peaks at ∼220 and ∼300 cm^{-1} in the IINS spectrum (see Figure 2). Adopting a similar approach, Prask et al.[7] have calculated their IINS spectrum by using a larger O−O strength force constant to strengthen the maximum optic frequency to ∼300 cm^{-1}. The peak at ∼220 cm^{-1} was produced in a similar way as Shawyer and Dean's calculations for the smaller sizes of the ice lattice (see later section). However, when a complete BZ integration over all

TABLE 1: Some Basic Properties of Water−Water Potentials

type of poten.	core repuls./dispers.	charge on H (*e*)	point charge	r_{om}[a] (Å)	force constant (eV/Å)[b]				ratio
					A	*B*	*C*	*D*	*B*:*D*
ST2	r^{-12}/r^{-6}	0.236	4/5	0.80	1.993	2.347	2.223	1.892	1.24
LS	r^{-12}/r^{-6}	0.330	3/3		1.311	1.691	1.492	1.318	1.29
KKY	exp/exp	0.400	3/3		1.144	1.233	1.175	1.081	1.14
Watts	exp/exp	0.329	3/3		0.921	1.073	1.027	0.920	1.18
TIPS2	r^{-12}/r^{-6}	0.535	3/4	0.15	0.846	0.923	0.947	0.846	1.12
RSL	exp/exp	0.330	3/3		0.834	0.829	0.828	0.833	1.01
TIP4P	r^{-12}/r^{-6}	0.520	3/4	0.15	0.779	0.866	0.827	0.773	1.12
TIP3P	r^{-12}/r^{-6}	0.417	3/3		0.783	0.809	0.794	0.703	1.15
Rowlinson	r^{-12}/r^{-6}	0.328	4/5	0.26	0.679	0.788	0.748	0.633	1.24
RSL2	exp/exp	0.330	3/3		0.520	0.539	0.523	0.510	1.05
MCY	exp/exp	0.718	3/4	0.26	0.272	0.293	0.286	0.259	1.13

[a] r_{om} is the separation distance of the position of the negative charge from the position of oxygen. [b] The force constants were calculated for water dimer with four different orientations, as shown in Figure 1: *A* is for the configuration of the dipole moments having a relative angle of 60°; *B* is for dipole moments having a relative angle of 180°; *C* is for 120°; *D* is for 0°. [c] The ratio of *B*:*D* provides the maximum difference among the four different force constants.

TABLE 2: Comparison of Force Constants Used in LD Models (Unit for *K, k* is eV/Å^2 and for *G, g* is eV/θ^2)[a]

		Shawyer−Dean[5]	Prask et al.[7]	Wong−Whalley[6]	Renker[8]	Bosi et al.[24]	our model[1]
k_1	O−H	33.58	33.9			38.7	36.1
k_2	H−H	−1.17				−1.8	−1.2
K_1	O- - -H	0.74	1.64	1.83/1.56/1.78/1.49	1.5/2.1	1.8	1.1/2.1
g_1	H−O−H	4.57	3.55			4.1	3.2
G_1	H−O- - -H	0.148	0.50			0.31	0.78
G_2	H−O- - -O	0.148	0.26	0.3	0.31/0.4	0.62	0.61
G_3	H- - -O- - -H			−0.34		0.65	0.45

[a] *k* and *g* are the internal stretching and bending force constants; *K* and *G* are the external stretching and bending force constants. The values for K_1 are the hydrogen-bonding force constants; some models have two force constants, and the Wong−Whalley model has four.

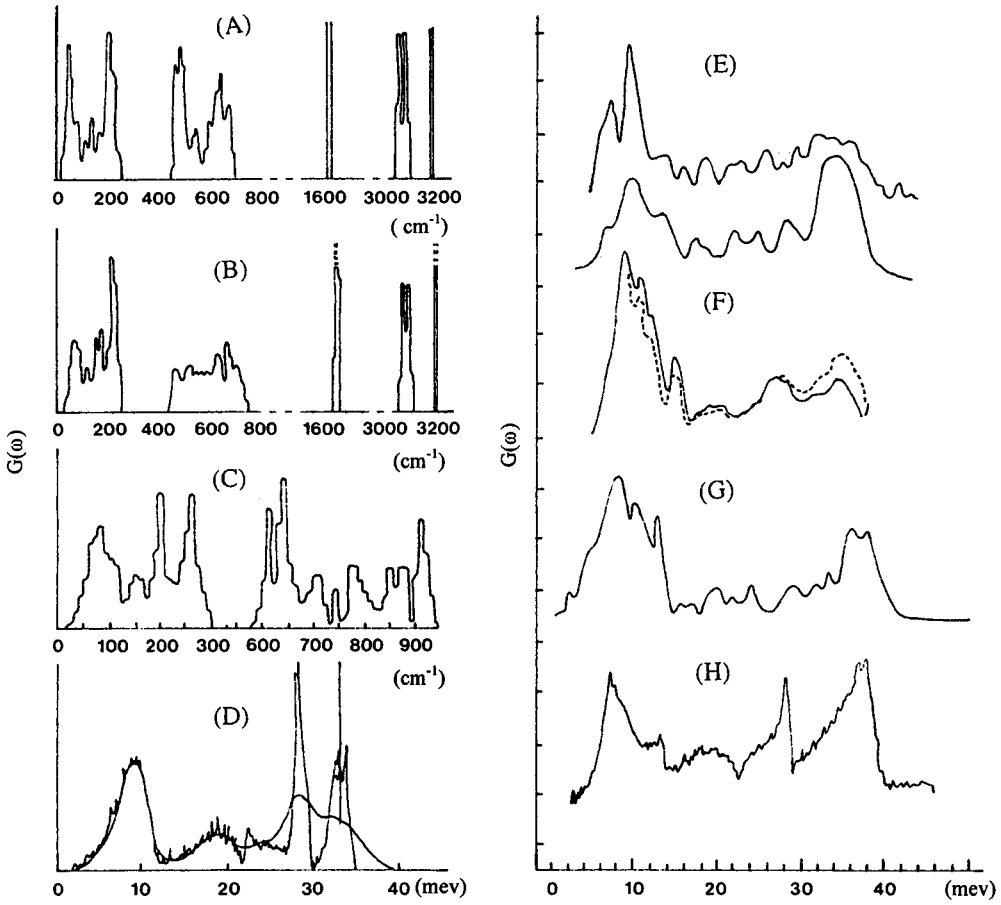

Figure 2. Comparison with LD and MD calculations by (A) Bosi et al.;[24] (B) Shawyer and Dean;[6] (C) Prask et al.;[7] (D) Renker;[8] (E) there are two curves: the upper one is the lattice dyamical calcution and the lower one is the molecular calculation (Marchi et al.[13]); (F) Sciortino and Corongiu;[17] (G) Burnham et al.;[16] and (H) experimental spectrum for ice Ih[1] (energy unit: 1 meV = 8.05 cm^{-1}).

the modes was made for the comparison, one can see that there is only one peak dominating the spectrum at ∼300 cm^{-1} (see Figure 2). Hence, these models were not in agreement with the measured IINS spectrum.

With the increase of performance of neutron spectrometers, the two peaks in the optic region have become clear. Renker[8] has measured the inelastic coherent neutron scattering and has shown that the two peaks in the translational region are much sharper. In order to represent the data measured, he proposed another model, which was based on an ordered proton model for ice Ih, where the O−O stretching force constant along the *c*-axis is approximately 1.7 times larger than the stretching force constant in the basal plane. This model predicts the two peaks in the PDOS (see Figure 2). However, our detailed study of this model found that the peak at ∼37 meV (298 cm^{-1}) in the calculated polarized spectra exists along the *c*-axis only, while the PDOS integrated over all the vibrational amplitudes in the basal plane only has one peak at ∼27 meV (225 cm^{-1}). Thus, this model is incompatible with our IINS spectra measured in these two orientations of ice Ih,[1] which shows that the peaks at about 28 and 37 meV do not depend on the orientation of the crystal. The recent LD calculation by Criado et al.[9] could also belong to this category.

An alternative explanation of the two peaks in the translation region based on TO/LO splitting has been proposed by Klug and Whalley.[10] They suggested that the two peaks are due to TO/LO splitting, as seen in ionic crystals, such as NaCl. There were some disagreements as to whether the idea of TO/LO splitting is valid for ice, because the argument for it depends on the existence of long-range charge interactions and has no calculations to back it up. However a number of strong arguments against this theory have emerged as a result of our recent measurements on a range of different ice structures using

IINS. Hence the consensus on this matter[11,12] is that the two peaks are not due to TO/LO splitting.

The second category of calculations was made by the use of MD techniques. One of the advantages of the MD method is that one can use "proper" pair potentials to calculate the PDOS, although modern LD programs are capable of adopting the effective potentials or using a range of force constants for the longer range interactions, such as the second-and the three-neighbor interactions. It is often that only the nearest neighbor interactions were taken into account. In fact, in most cases the nearest neighbor interactions are the predominant term affecting vibrational frequencies. Because of this simplification, the LD calculations can produce a very high quality of PDOS without resorting to powerful computers. On the other hand, for MD calculations, a very large supercell has to be used to produce a modest quality PDOS. This is because MD calculates modes at $q = 0$ and the other modes in the first BZ can only be included by the "folding" effect. This means that in order to include the BZ boundary points, the size of the cell will be at least $2 \times 2 \times 2$ (=8 primary cells, 32 water molecules). The result of this calculation cannot be considered an "accurate" representation of the integrated PDOS for the comparison of IINS data, because it contains only *q*-points at the BZ center and boundary. We believe that the minimum requirement for MD calculations of PDOS is $4 \times 4 \times 4$ (=64) cells (this gives one *q*-point in the middle of the first BZ along each principle direction), which means that at least 256 water molecules are needed for ice Ih structure, and a larger cell, $8 \times 8 \times 8$ (=320, i.e. 1280 water molecules), is more desirable. Even so, this calculation is equivalent only to the LD calculation of 5 *q*-points in each direction (i.e. total $5 \times 5 \times 5$ *q*-points in the first BZ). A typical LD calculation could be $50 \times 50 \times 50$ *q*-points in the first BZ (i.e. 3 orders of magnitude better in terms of the mode integration). One of early MD calculations for ice was carried out by Marchi et al.[13] using a simple point charge rigid-molecule potential for ice Ih (with 128 water molecules). The MD result from their calculations was compared with that of their LD calculations using the same potential and cells; the results show similar features, a peak at 260 cm^{-1}, but with poor statistics for the MD calculations. These results have been used for the interpretation of their IR data.

Recently there has been renewed interest for MD calculations of ice Ih, partially due to the increased computing power available. One such calculation was done by Itoh et al.,[14] who used a "real" potential developed by Kumagai et al.[15] using 350 molecular cell. This potential is one of the nonrigid water potentials with an extra three-body term for H−O−H and H−O- - -H bending. As a result, their calculations produced not only the translational modes but also the librational modes and internal strengthening and bending modes up to 3500 cm^{-1}. Because a slightly larger cell was used in our calculations using the same potential,[16] the PDOS spectrum is much better in comparison with Itoh et al.'s calculation.[14] The most significant feature of the calculated result, as we can see, is that there is still one peak for the molecular optic modes at 300 cm^{-1} for both calculations.[14,16] This is again inconsistent with IINS data. Using a polarized potential developed from the MCY potential, Sciortino and Corongiu[17] have calculated the PDOS for ice Ih in the translational region with a cell of about 300 molecules. The calculation has reproduced two peaks at 210 and 270 cm^{-1}. We believe that it could be due to the similar effect seen in Shawyer and Dean's calculation: the incomplete summation of the first BZ, which can also be seen from the poor quality of the acoustic band calculated, since this band is independent of the model used (it is dominated by the O−O−O bending force constant). A good integration of the first BZ will always produce the shape of the acoustic band similar to IINS data, as shown from Ranker's (LD)[8] and Itoh et al.'s (MD)[14] calculations. We therefore wish to emphasize that the comparison with IINS data should be made by using an integrated PDOS; one should not look for each individual mode calculated for the comparison. This is the fundamental difference between neutron scattering and IR/Raman techniques.

4. The Size Effect from Lattice Dynamic and Molecular Dynamic Calculations

In order to understand the basic properties of LD and MD calculations for phonons, we have made a series of studies of some of the basic properties of dispersion curves vs PDOS. Figure 3 shows the typical dispersion curves calculated for the ice Ih and Ic using Prask et al.'s model (the force constants used are listed in Table 2). We chose Ic for the demonstration, because it can be constructed with a minimum number of molecules in the primary cell (i.e. 2 molecules), and in contrast, at least 4 molecules are needed for ice Ih. The lower curves are the density of states integrated along the three particular directions [111], [110], and [100]. As one can see, although this model has only one H-bond force constant, it shows two peaks at 180 and 230 cm^{-1} when the integration is incomplete. In fact, the peak at 220 cm^{-1} is due to the LO mode at boundaries of the [110] and [100] directions. The upper curves in Figure 3 show a series of calculations of the structure with different *q* mesh points, starting with $2 \times 2 \times 2$. When more *q*-points are summed in the BZ, this peak at 220 cm^{-1} becomes less intense relative to the peak at 310 cm^{-1}. Eventually it completely submerged in the background. This process is also applicable to the calculations for Ih as indicated in Figure 3. When a pair potential is used, we have demonstrated that the dispersion curves do not show a drastic difference in comparison with the force constant model.[16]

One of the interesting questions is why it is not possible for existing potentials to produce the measured spectrum for ice Ih, despite the fact that they include long-range interactions and produce some degree of orientational differences (see Table 1) in the energy surfaces. Regarding the long-range interaction in ices, we believe that the effect is much smaller than people have imagined. It is evident that, firstly, the IINS spectrum for ice in small pores (average diameters 10−30 Å) is very similar to the ice spectrum for bulk.[18] A small difference can be seen only in the left-hand cutoff of the librational band (at 68 meV), which is due to the surface molecules. Water molecules in such small pores have neighbors not more than three neighboring distances on average; secondly, the similarity of the translational modes for ice Ic, Ih, and low-density amorphous ice indicates that the peaks are also irrelevant to the long-range arrangement of the molecules (or structures). This implies that phonon frequencies are predominately determined by the nearest neighbor interactions. According to structural simulations, the longer range interactions would push molecules closer. As long as the structure is relaxed, the vibrational frequencies will be effectively determined by the derivative of the pair potential at the separation distances; this is true at least for the modes having long wavelengths, i.e. at $q = 0$. As we know, the most commonly used potentials today (listed in Table 1) give some degree of differences in the force constants along different orientations, as illustrated in Figure 1. However, if the force differences for the different orientations (shown in Figure 1A,B,C,D) are small, the modes can not be decoupled from one motion to another. Hence, the optic modes become a broad band without splitting, as shown in the measured spectrum.

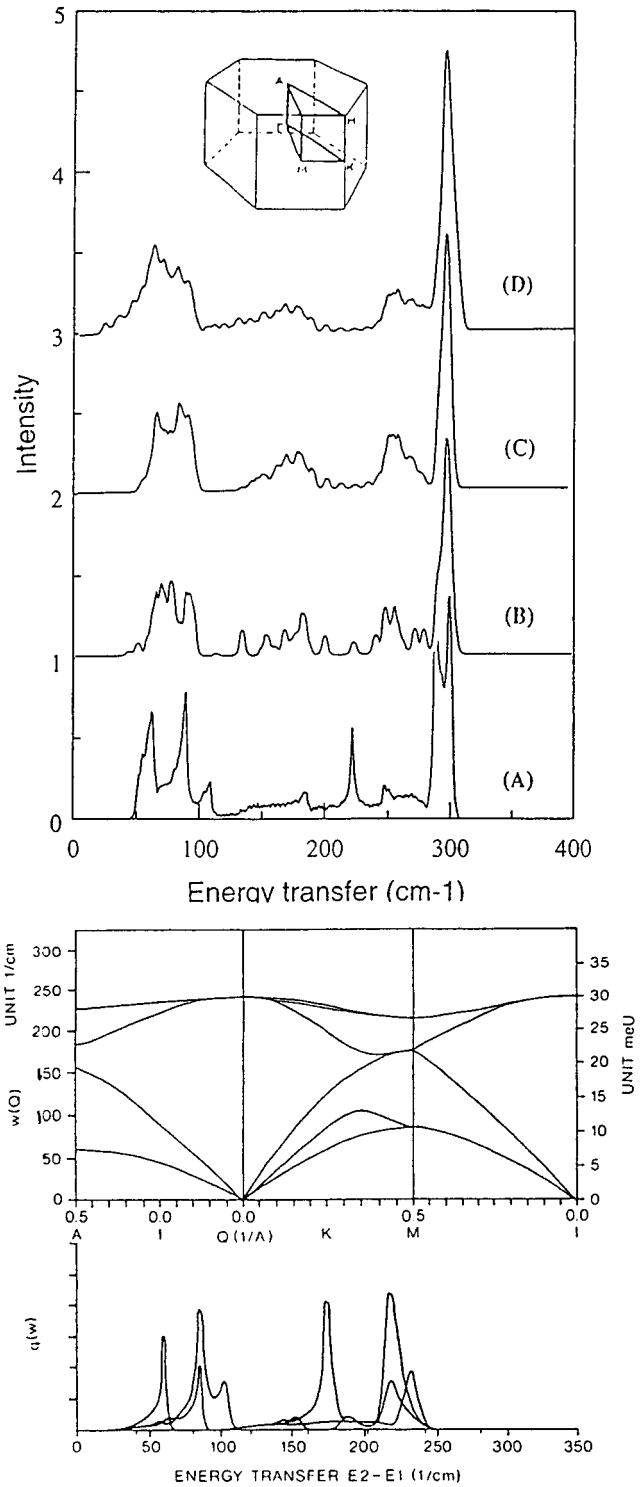

Figure 3. (Two lower diagrams) Dispersion curves and $G(\omega)$ calculated for these three principal directions using our model described in Table 1. (Upper diagrams) Series of calculations of $G(\omega)$ using the same model with different density of the q-points in the BZ integration. Curve A is integrated over $2 \times 2 \times 2$ q-points in the first BZ; curve B is for $3 \times 3 \times 3$ q-points; curve C is for $4 \times 4 \times 4$ q-points; and curve D is for $10 \times 10 \times 10$ q-points. The calculations show that the peak at 28 meV consists of a very small number of modes near the BZ boundary, and it does not constitute the main peak (or intensity) in the complete, integrated $G(\omega)$.

In order to illustrate this point, we have made a series of calculations for the PDOS with different ratios of K_1:K_2.[23] The results show that for the PDOS with a ratio less than 1.5 the optic modes still show no sign of splitting. This implies that the splitting phenomena can only be seen when the ratio of the strong/weak force constants among the nearest neighboring molecules is greater then 1.5. As we indicated in the earlier section, the potential we have tested so far shows that the ratios are all less than this value. Indeed, if we assume that the orientational differences come only from the charge terms based on the classic considerations, including polarized potentials, it would be almost impossible to get a greater ratio.

5. The Two Strengths of the Hydrogen Bond Model

In order to explain all the properties of the IINS spectra of ice, we conclude that the two molecular peaks are associated with different local dipole−dipole configurations. We postulate that the relative intensities of the two optical bands are entirely dependent on the relative number (or ratio) of these configurations which are related to the strong and weak H-bonds in the ice structure. For instance, in ice Ic (which has an identical IINS spectrum to ice Ih), the protons are completely disordered. Hence, statistically, it has one of the C configurations to every two of the D configurations. Therefore, in ice Ic, there will be one weak H-bond for every two strong H-bonds (ratio is 1/3: 2/3). They are randomly and isotropically distributed in the ice structure, which gives the integrated peak area for the low-energy/high-energy optic modes in a ratio of about 1:2, as observed. The weak/strong force constants used in the calculation are 1.1 and 2.1 eV/Å, and their ratio is 1.9 in comparison with the maximum, 1.3, for all existing potentials (see Table 1). The difference of the two H-bond force constants is considerably larger than can be explained on the basis of electrostatic effects only.

Since the large differences of force constants used in the LD calculations cannot come from static charge interactions, an important question would be what is the cause of the further splitting of the force constant. As we know, the hydrogen bond interactions are not only interactions from the positively charged H atoms to the negatively charged O atoms; there is also a small element of covalence. Its asymmetrical molecule combined with the fact that the electrons in the 2s and 2p orbitals of the O atom can be easily rehybridized to respond to the changes of the distances of adjacent molecules could allow the H-bonds to exist in two different electronic states. This may even affect the internal O−H covalent bond strength. Ab initio water dimer calculations frequently indicate that the interactions between the two molecules are sensitive to the relative orientations of the molecules. For different configurations (or relative orientations), the ab initio calculations show they have different bonding energies and O−O separation distances.[19] The configuration D is the most energetically stable one (having a short O−O bond length). The differences in terms of force constants are significantly larger than that given from the classic potentials. Recently, ab initio calculation results for a larger water cluster showed that the difference among the different orientations will increase when the two water molecules are actually fully connected.[19] This is not surprising, because only when all four hydrogen bonds for each water molecule are connected can rehybridization occur, and as a consequence, the hydrogen bond may split into two groups.

6. Discussion

The assumption of two strengths of H-bonds in ice is the unavoidable conclusion, considering all the attempts of reproducing the PDOS for ices in the past. It is also a logical extension of our understanding of the polarized nature of water−water potentials. There are many other defects associated with the potentials listed in Table 1, such as the lack of restriction of bending motion, which makes it almost impossible for these

potentials to produce the right frequencies for the librational modes (this has been overcorrected by introducing a three-body term in the potential proposed by Kumagai et al.[14]), and this area also requires our further attention.

Recently, we have made great efforts in ab initio calculations to try to find the source of the large force constant splitting. These calculations will have to be done in the fully connected lattices, as we indicated above. Because the ab initio calculates total energy of the system, it is difficult to calculate the bonding energy and force constant for each individual pair in the lattice. However, from a number of independent ab initio calculations,[19,20] one can see that the O−O separation distances are different from one configuration to another and they tend to separate into two groups at 2.74 and 2.76 Å. This is in agreement with neutron diffraction measurements made by Kuhs et al.[21]

If our hypothesis is correct, the implications are that it not only provides a mechanism to explain a wide range of abnormal behavior of water but also casts new light on our understanding of the polymorphism of ice, for instance, why the $T-P$ phase diagram of ice is so complicated and what energy difference exists between ice Ih and Ic. The reason is because the strong and weak bonds are of different bond lengths, which would mean that some bonds are compressed while others are stretched. One can assume that when external pressure is applied, the different types of configurations (or bond types) respond to the pressure differences. This implies that some forms of bonds become relatively more stable than others under pressure. We therefore believe that the disordered forms of ice (with a mixture of the strong and weak bonds) are a frustrated system. This stress energy is also capable of accounting for the small energy difference between ice Ih and Ic, because ice Ih has an extra lattice parameter, c, which can be optimized in response to the surrounding stress. Therefore, the total free energy for ice Ih is lower than that of ice Ic, and it can be reduced further when proton ordering in the system increases, such as the case in ice XI. The c/a ratio decreases from 1.628 for ice Ih to 1.617[22] in comparison with the value of 1.632 from the cubic structure of ice Ic.

An interesting question one would ask is that if the strong H-bond corresponds to the lower energy state, why ordinary ice Ih does not form a structure with only strong bonds and become a fully ordered system. The reason for this is that the energy difference between the two types of H-bonds is relatively small (although the difference of force constants is large) compared with the entropy contribution from the asymmetrical water molecules, $TS_0 = \mathrm{TK}\ \ln(3/2)$ at 100 K or above, causing the proton disordering and hence the two kinds of bonds to be completely randomly distributed in most structures of ice. This mixture (having short and long bonds) causes distortion of the O positions, as observed by neutron diffraction.[14] This may be the reason why some H's in the disordered structures of ice are compressed away from the straight lines of O- - -O. This internal stress could have a large effect on the stability of the structure, which was not considered in the past.

Acknowledgment. The author thanks the Engineering and Physics Science Research Council (EPSRC), U.K., for financial support and the Rutherford Appleton Laboratory for the use of neutron facilities.

References and Notes

(1) Li, J.-C.; Ross, D. K. *Nature* **1993**, *365*, 327. Li, J.-C. *J. Chem. Phys.* **1996**, *105*, 6733.
(2) Finney, J. L.; Quinn, J. E.; Baum, J. O. In *Water Science Review; Franks, F., Ed.; Cambridge University Press: Cambridge, 1985; Vol. 1, p 93.*
(3) Morse, M. D.; Rice, S. A. *J. Chem. Phys.* **1982**, *76*, 650.
(4) Matsuoka, O.; Clementi, E.; Yoshimine, M. *J. Chem. Phys.* **1976**, *61*, 1351.
(5) Shawyer, R. E.; Dean, P. *J. Phys. C* **1972**, *5*, 1028.
(6) Wong, P. T. T.; Whalley, E. *J. Chem. Phys.* **1976**, *65*, 829.
(7) Prask, H. J.; Trevino, S. F.; Gault, J. D.; Logan, K. W. *J. Chem. Phys.* **1972**, *56*, 3217.
(8) Renker, B. In *Physics and Chemistry of Ice*; Whalley, E., Hones, S. J., Gold, L. W., Eds.; University of Toronto Press: North York, ON, 1973; p 82.
(9) Criado, A.; Bermejo, F. J.; Carcia-Hernandez, M.; Martinez, J. L. *Phys. Rev E* **1992**, *47*, 3516.
(10) Klug, D. D.; Whalley, E. *J. Glaciology* **1978**, *21*, 55. Comment: *J. Chem. Phys.* **1979**, *71*, 1513.
(11) Klug, D. D.; Tse, J.; Whalley, E. *J. Chem. Phys.* **1991**, *95*, 7011. Tse, J. S. Private communication.
(12) Li, J.-C.; Ross, D. K. *J. Phys. Condens. Mater*. **1994**, *6*, 10823.
(13) Marchi, M.; Tse, J. S.; Klein, L. *J. Chem. Phys.* **1986**, *85*, 2414.
(14) Itoh, H.; Kawamura, K.; Hondoh, T.; Mae, S. *Physica B* **1996**, *219&220*, 469.
(15) Kumagai, N.; Kawamura, K. K.; Yokokawa, T. *Mol. Simul.* **1994**, *12*, 177.
(16) Birnham, C. J.; Li, J. C.; Leslie, M. *J. Phys. Chem.* **1997**, *101*, xxx.
(17) Sciortino, F.; Corongiu, G. *J. Chem. Phys.* **1993**, *98*, 5694.
(18) Li, J. C.; Bennington, S. M.; Benham, M. J.; Ross, D. K.; Tomkinson, J. In *IOP Conference Series (U.K.)* **1989**, *101*, 109.
(19) Heggie, M.; Maynard, S. *Chem Phys. Lett.* **1996**.
(20) Morrison, I.; Li, J.-C.; Xanthean, S. S.; Payne, M. *J. Phys. Chem.* **1997**, *101*, xxx.
(21) Kuhs, W. F.; Finney, J. L.; Vettier, C.; Bliss, D. V. *J. Chem. Phys.* **1984**, *81*, 3612.
(22) Howe, R.; Whitworth, R. W. *J. Chem. Phys.* **1989**, *90*, 4450.
(23) Li, J.-C.; Leslie, M. *J. Phys. Chem.* **1997**, *101*, xxx.
(24) Bosi, P.; Tubino, R.; Zerbi, G. *J. Chem. Phys.* **1973**, *59*, 4578.